

Serotype O:8 isolates in the *Yersinia pseudotuberculosis* complex have different O-antigen gene clusters and produce various forms of rough LPS

Johanna J Kenyon¹, Katarzyna A Duda², Antonia De Felice³,
Monica M Cunneen¹, Antonio Molinaro³, Juha Laitinen⁴,
Mikael Skurnik^{4,5}, Otto Holst², Peter R Reeves¹ and
Cristina De Castro⁶

Abstract

In *Yersinia pseudotuberculosis* complex, the O-antigen of LPS is used for the serological characterization of strains, and 21 serotypes have been identified to date. The O-antigen biosynthesis gene cluster and corresponding O-antigen structure have been described for 18, leaving O:8, O:13 and O:14 unresolved. In this study, two O:8 isolates were examined. The O-antigen gene cluster sequence of strain 151 was near identical to serotype O:4a, though a frame-shift mutation was found in *ddhD*, while No. 6 was different to 151 and carried the O:1b gene cluster. Structural analysis revealed that No. 6 produced a deeply truncated LPS, suggesting a mutation within the *waaF* gene. Both *ddhD* and *waaF* were cloned and expressed in 151 and No. 6 strains, respectively, and it appeared that expression of *ddhD* gene in strain 151 restored the O-antigen on LPS, while *waaF* in No. 6 resulted in an LPS truncated less severely but still without the O-antigen, suggesting that other mutations occurred in this strain. Thus, both O:8 isolates were found to be spontaneous O-antigen-negative mutants derived from other validated serotypes, and we propose to remove this serotype from the O-serotyping scheme, as the O:8 serological specificity is not based on the O-antigen.

Keywords

O-Antigen, O-specific polysaccharide, O:8 serotype, serotyping, *Yersinia pseudotuberculosis*

Date received: 21 October 2015; revised: 8 January 2016; accepted: 13 January 2016

Introduction

LPS is a lipoglycan present on the cell surface of most Gram-negative bacteria. For many pathogens, including *Yersinia pseudotuberculosis*, the LPS is an important virulence determinant.^{1–3} The structure is comprised of three key segments: lipid A, which anchors the structure in the outer membrane; the core oligosaccharide, consisting of inner core and outer core sections; and, usually, O-specific polysaccharide (OPS; also known as the O-antigen). The OPS is composed of variable-length polymers of repeating oligosaccharide units (O units) that often vary in structure within a species. The different forms are classically differentiated using serology, and the O-serotyping scheme for *Y. pseudotuberculosis* currently defines 21 different O-serotypes.⁴ Recently, it was proposed that this serotyping scheme can be

¹School of Molecular Bioscience, University of Sydney, Sydney, NSW, Australia

²Division of Structural Biochemistry, Research Center Borstel, Leibniz-Center for Medicine and Biosciences, Borstel, Germany

³Department of Chemical Sciences, University of Napoli, Napoli, Italy

⁴Department of Bacteriology and Immunology, Medicum, and Research Programs Unit, Immunobiology, University of Helsinki, Helsinki, Finland

⁵Helsinki University Central Hospital Laboratory Diagnostics, Helsinki, Finland

⁶Department of Agriculture Sciences, University of Napoli, Portici, Italy

†Johanna J Kenyon and Katarzyna A Duda contributed equally
Current address for Johanna J Kenyon: School of Biomedical Sciences, Queensland University of Technology, Brisbane, QLD, 4001, Australia

Corresponding author:

Cristina De Castro, Department of Agriculture Sciences, University of Napoli, Via Università 100, 80055 Portici (NA), Italy.
Email: decastro@unina.it

applied to all members of the *Y. pseudotuberculosis* complex, which also includes *Y. pestis*, *Y. similis* and *Y. wautersii*.^{5,6}

The majority of genes that are required for the synthesis, assembly and processing of O-unit structures in the *Y. pseudotuberculosis* complex are in a gene cluster flanked by conserved *hemH* and *gsk* genes.⁷ The OPS gene clusters and corresponding O-unit structures of 18 serotypes have been determined.⁸ Many *Y. pseudotuberculosis* OPS gene clusters contain a *ddhDABC* gene set encoding for a precursor common to most of the rare immunodominant 3,6-dideoxyhexose (3,6-DDH) sugars that are always attached as a side-branch of the O-unit structure.⁹ Seven different 3,6-DDH sugars, five hexoses and two octoses branched at C-4 (yersinose A and B), have been found in the *Y. pseudotuberculosis* complex.⁹ These sugars include paratose, tyvelose (Tyvp) and abequose, which are also found in *Salmonella enterica*.¹⁰ The type of 3,6-DDH sugar produced is determined by one or two *ddh*-specific genes located immediately downstream of *ddhDABC* in the OPS gene cluster, being *prt*, *prt* and *tyv*, and *abe*, respectively, for paratose, Tyvp and abequose.

OPS gene clusters include *wzx*, *wzy* and *wzz* genes that encode proteins involved in the Wzx/Wzy-dependent processing pathway.⁷ In this pathway, the OPS is made by polymerization of an oligosaccharide O unit, and in *Y. pseudotuberculosis*, O-unit synthesis is initiated by the transfer of *N*-acetyl-D-glucosamine phosphate from UDP-D-GlcPNAc to the inner-membrane lipid carrier, undecaprenyl phosphate (UndP), by the WecA initial transferase. This is followed by glycosyltransferase enzymes sequentially adding the remaining sugars. If the Gnu enzyme is present, UndPP-D-GlcPNAc can be converted to UndPP-*N*-acetyl-D-galactosamine (UndPP-D-GalpNAc), so that GalpNAc replaces GlcPNAc as first sugar.^{11,12} The Wzx translocase flips the O unit to the periplasmic face of the inner membrane for polymerization by the Wzy polymerase. Wzz regulates the length of the OPS polymer before ligation to the lipid A core.¹³ Historically, isolates that produce long-chain OPS polymers have been described as 'smooth', while isolates with LPS structures devoid of OPS (i.e. only the lipid A and core oligosaccharide segments) are described as 'rough'. The structure of the lipid A and of the core oligosaccharide is reported for several *Yersinia* species,⁸ and those from *Y. pseudotuberculosis* and *Y. pestis* share many structural features, because this last species evolved from the former approximately 1500–20,000 yr ago.¹⁴ As many other *Enterobacteriaceae*, the lipid A from *Y. pseudotuberculosis* presents the classical glucosamine disaccharide linked β -(1→6), capped with a phosphate at both ends, and acylated with long chain fatty acids (Figure 1). The number and the type of fatty acids, along with the presence of other substituents, such as phosphoethanolamine, 4-amino-4-deoxy-L-arabinose or

additional phosphate groups, depends strictly on the growing conditions or from the environmental milieu and it is regulated from the PhoP-PhoQ regulation system.¹⁵

The core region contains a conserved hexasaccharide, constituted by two Kdo residues (named inner and external), three L,D-Hep units (each annotated with a roman numeral) and one Glc (Figure 1).¹⁶ Variations on this conserved structure depend again on growth conditions and may involve replacement of the external Kdo with a different octonic acid, D-glycero-D-talo-oct-2-ulopyranosylonic acid or Ko, elongation at Hep III with a D,D-Hep or with a Gal residue, while Hep II is the point of attachment of the O-antigen.^{16,17}

The serological typing system for *Y. pseudotuberculosis* was developed in stages, and there have also been changes to the nomenclature. Six serogroups (I–VI) were established prior to 1984, as described by Tsubokura et al.¹⁸ Two new ones, VII and VIII, were then proposed in 1984,¹⁸ and the use of Roman numerals was replaced with an Arabic numbering system (O:1–O:8), with some groups having subtypes, for example O:1a and O:1b.¹⁹ Serogroups O:9–O:15 were described in updates to the typing scheme.^{4,20} However, we now treat all as serotypes, as there is no further subdivision into serovars in *Y. pseudotuberculosis*.

The history of serotype O:8 is unusual. The first report of this serotype stated that the type strain (isolate 151) expressed only one epitope, O factor 20, that was unique to O:8,¹⁸ but the 1993 revision of the scheme reported that the O:8 type strain has a rough phenotype,²⁰ that is, did not produce OPS, and this was not further investigated. In the following update, O:8 isolates were reported to react with O factor 11,⁴ which had previously been described for serotypes O:2c and O:4a.¹⁹ We now know that serotypes O:2c and O:4a have an O antigen with the same main chain,⁹ which implies that epitope 11 is in the shared portion of the O-antigen structure. However, cross-reaction of epitope 11 with O:8 conflicts with the previously reported 'rough' phenotype. In this study, we examine the OPS gene clusters and LPS products by two O:8 isolates.

Materials and methods

Bacterial strains and growth

Yersinia pseudotuberculosis isolates 151 (O:8 type strain) and No. 6 used in this study have both been described previously.^{4,18} All strains and plasmids used in this study are listed in Table 1. Bacteria were routinely grown in Luria broth (LB) or on Luria agar; for fermentor cultivation, a 250-ml inoculum in LB was grown overnight at 25°C on a rotary shaker at 200 rpm. Fermentor cultivation was done in a BIOSTAB B plus Santorius Fermentor with 4 l *Yersinia* fermentor

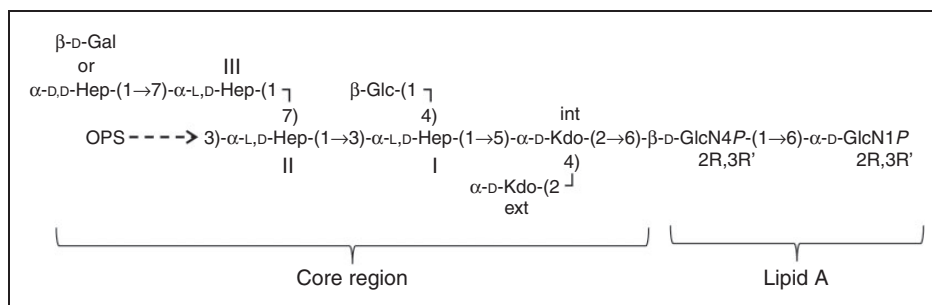


Figure 1. Representation of the main form of the carbohydrate backbone of the lipopolysaccharide from *Y. pseudotuberculosis*. Variations in the core region occur at different level: the external Kdo can be replaced by Ko, while Hep III can have either a D,D-Hep or a Gal residue. Hep II is the site of attachment of the O₂ antigen or OPS.

Table 1. Bacterial strains and plasmids used in this study.

Strain/plasmid	Characteristics	Source/reference
<i>Y. pseudotuberculosis</i>		
151	<i>Y. pseudotuberculosis</i> serotype O:8	17
151/pPR2161	<i>Y. pseudotuberculosis</i> 151 + pPR2161	This study
No. 6	<i>Y. pseudotuberculosis</i> serotype O:8	Skurnik laboratory strain collection obtained from Hiroshi Fukushima
No. 6/pSW23T-waaF6	<i>Y. pseudotuberculosis</i> No. 6 + pSW23T-waaF6	This study
1261/79	<i>Y. pseudotuberculosis</i> serotype O:3	44
51	<i>Y. pseudotuberculosis</i> serotype O:4a	4
IP32953	<i>Y. pseudotuberculosis</i> serotype O:1b	45
Other strains		
<i>E. coli</i> JM109	<i>endA1</i> , <i>recA1</i> , <i>gyrA96</i> , <i>thi</i> , <i>hsdR17</i> (<i>r_k⁻</i> , <i>m_k⁺</i>), <i>relA1</i> , <i>supE44</i> , Δ (<i>lac-proAB</i>), [<i>F'</i> <i>traD36</i> , <i>proAB</i> , <i>laqI^qZ</i> Δ M15]	Promega
<i>E. coli</i> ω 7249	B2163 Δ nic35, <i>E. coli</i> strain for suicide vector delivery, requirement for diaminopimelic acid, Km ^R	46
YeO3-R1	Spontaneous rough <i>Y. enterocolitica</i> O:3 mutant	47
YeO3-R1-M164	YeO3-R1 (<i>waaF::CatMu</i>)	42
Plasmids		
pTrc99A	High copy number expression vector with multiple cloning sites (MCS) following IPTG inducible <i>P_{trc}</i> promoter. Amp ^R	Promega
pSW23T	Suicide vector with multiple cloning sites (MCS) with <i>oriT_{RP4}</i> and <i>oriV_{R6Kγ}</i> . Cml ^R Clm ^R	31
pPR2161	pTrc99A with <i>Y. pseudotuberculosis</i> O:4a <i>ddhD</i> inserted at <i>NcoI</i> and <i>BamHI</i> sites. Amp ^R .	This study
pSW23T-waaF6	pSW23T with <i>Y. pseudotuberculosis</i> O:1b <i>waaDFC</i> operon inserted between <i>BamHI</i> and <i>HindIII</i> sites. Clm ^R .	This study

IPTG = isopropyl β -D-thiogalactopyranoside.

medium as described elsewhere.²¹ During fermentation pH was maintained at 7.4 by addition of 20% NaOH. The pO₂ of the culture was kept at 50% saturation by sterile air-flow aeration and stirrer speed control. After 24 h fermentation at 25°C, the bacteria were killed by a final concentration of 1% phenol, washed with PBS until the supernatant was clear and freeze-dried.

Isolation of LPS

The bacteria (52.8 g and 11 g, strains No. 151 and 6, respectively) were washed successively with ethanol, acetone and ether. De-lipidated bacterial masses (9.96 g and 3.85 g, strains No. 151 and 6, respectively) were extracted with hot phenol/water (2.49 g and 430 mg crude LPS, 25% and 11.2% of bacterial dry mass,

strains No. 151 and 6, respectively).²² The obtained water phases were dialysed, then lyophilized and purified by enzymatic treatment,²³ then dialysed and lyophilized. The samples were ultracentrifuged (150,000 g, 4°C, 4 h) three times, then lyophilized (yield of pure LPS: 4.3% and 6% for 151 and 6, respectively).

General and analytical methods

Chemical composition analyses of LPS included P, Kdo and GlcN determination, as well as methanolysis (0.5 M HCl/MeOH, 85°C, 45 min.)^{24,25} and neutral sugar analysis as previously described.²⁶ All analyses were performed in duplicates.

Isolation of oligosaccharides 1, 2 and 3

LPS was dissolved in anhydrous hydrazine (25 mg/ml), stirred at 37°C for 30 min, cooled, poured into ice-cold acetone (20 ml) and allowed to precipitate. The precipitate was then centrifuged (3000 g, 30 min, 4°C), washed twice with ice-cold acetone, dried, and then dissolved in water and lyophilized. The sample was *N*-deacylated with 4 M KOH as described,²⁷ and desalted by gel-permeation chromatography [Sephadex G-10 (GE Healthcare Europe GmbH, Freiburg, Germany) 50 × 1.5 cm, in 10 mM NH₄HCO₃, flow 1 ml/min]. The resulting oligosaccharide fraction was further purified by HPAEC on a Carbpak PA-100 column (9 × 250 mm) eluted with a linear gradient of 20–50% of 1 M sodium acetate in 0.1 M NaOH at 2.0 ml/min over 130 min.

NMR spectroscopy

One-dimensional spectra were recorded with a Bruker DRX 600 spectrometer equipped with a z-gradients reverse probe, and chemical shifts were referred relative to internal acetone ($\delta^1\text{H}$ 2.225, $\delta^{13}\text{C}$ 31.5); two-dimensional (2D) NMR spectra of 1 and 2 were recorded in 0.5 ml ²H₂O at 32°C; 2D NMR spectra of oligosaccharide 3 were acquired at 25°C.

For the homonuclear experiment, solvent-saturated double quantum-filtered correlation spectroscopy (DQF-COSY), total correlation spectroscopy (TOCSY), transverse rotating frame overhauser enhancement spectroscopy (TROESY) spectra and 512 free induction decays (FID)s of 2048 complex data points were collected, with 48 scans per FID and using standard manufacturer software. The spectral width was set to 10 ppm and the frequency carrier was placed at the residual HOD peak; mixing times of 100 and 300 ms were used for TOCSY and TROESY, respectively. For the heteronuclear single quantum coherence (HSQC) spectrum, 512 FIDS of 2048 complex points were acquired with 50 scans per FID; the GARP sequence was used for ¹³C decoupling during acquisition. As for heteronuclear multiple bond correlation (HMBC) and HSQC-TOCSY, the

same resolution in the two dimensions was used, but scan number was doubled and tripled, respectively. Data processing and analysis was performed with the standard Bruker Topspin 3.0 program.

ESI-MS/IT-TOF spectrometry

Oligosaccharides 1, 2 and 3 were analyzed by ESI-MS analyses using an ESI-MS/IT-TOF instrument (Shimadzu Europe, Manchester, UK). Each sample was dissolved in aqueous solution at a concentration of 0.1 mg/ml, and 200- μ l aliquots were injected directly in ESI at flow rate of 0.2 ml/min. The quadrupole was scanned in positive and negative mode over 400–2000 *m/z* range. An electrospray voltage of 1.90 kV and a nitrogen gas flow of 1.5 l/min were employed. Mass calibration and tuning were performed according to the manufacturer's recommendations. The spectra were acquired using the LC MS Solution software; all mass values are reported as average masses, and deconvolution of mass spectra was performed using both Shimadzu deconvolution software and ESI prot software.

PCR, sequencing and bioinformatic analysis

Chromosomal DNA was extracted from representative isolates of O:1b and O:4a, and from isolates 151 and No. 6, using the ultra-pure method described previously.²⁸ The OPS gene cluster of No. 6 was typed by PCR using the genotyping scheme for *Y. pseudotuberculosis*.²⁹ The sequence of the 151 OPS gene cluster was obtained by a process of PCR walking from conserved *hemH* and *gsk* genes at either ends of the region, and also using primers designed from O:4a sequence. PCR products were sequenced using the AB3730xl sequencing platform carried out by the Australian Genome Research Facility (Sydney, Australia).

A consensus sequence was obtained for 151 by compiling sequence trace files, and bioinformatics analysis was performed as described previously.²⁸ Insertion sequences (IS) were identified and characterized using ISFinder (<https://www-is.biotoul.fr>). The final sequence for 151 was deposited into GenBank under accession number KM454907.

Cloning and complementation of *ddhD*

The *ddhD* gene was amplified from chromosomal DNA from strain 51 (O:4a) using high-fidelity PCR (described previously¹⁹) with primers that incorporated flanking *NcoI* (5') and *BamHI* (3') restriction sites into the product. The product and the pTrc99A expression vector (obtained from Promega, Madison, WI, USA)³⁰ were digested with *NcoI* and *BamHI*, and then ligated together according to the manufacturers instructions (New England Biolabs, Ipswich, MA, USA). The

sample was cloned into *Escherichia coli* K-12 JM109, for selection of positive constructs. A positive transformant was selected, and the constructed plasmid purified and confirmed by PCR and sequencing prior to electroporation into strain 151. Electroporation was conducted using a BioRad gene pulser with the following conditions: 25 μ FD, 25 kV, 200 Ohm. Expression of the *ddhD* gene in pTrc99A was induced by supplementing cultures with 1 mM isopropyl β -D-thiogalactopyranoside in exponential phase (OD_{600nm} 0.4), before harvesting cells at OD_{600nm} 0.7 for further analysis.

Cloning of *waaDFC* operon and complementation of the *waaF* mutation in strain No. 6

The 3407-bp DNA fragment carrying the *waaDFC* operon was amplified by PCR using genomic DNA of *Y. pseudotuberculosis* strain IP32953 as the template, and primers *waaF6-F* (5'-GCGaagcttGCTGATAAAAGG GGTGCTTG-3') and *waaF6-R* (5'- GCGggatcCGTT AGAGCTGTTGGGTGCT-3'), which contained the BamHI and HindIII restriction sites for cloning. The 1.8-kb suicide vector pSW23T,³¹ and the *waaDFC* fragment were digested with restriction enzymes BamHI and HindIII. The linearized pSW23T DNA was dephosphorylated by a 20-min FastAP alkaline phosphatase (Fermentas, Waltham, MA, USA) treatment at 37°C. The DNA fragments were ligated for 1 h at room temperature (RT) and 16 h at 4 °C. After ligation the DNA was ethanol-precipitated, solubilized into 10 μ l water and electroporated into *E. coli* ω 7249 cells. The transformants were plated on LA plates containing 0.3 mM diaminopimelic acid (DAP), 20 μ g/ml chloramphenicol and 100 μ g/ml kanamycin. The obtained colonies were checked for the presence of the insert PCR using insert primers *waaF6-F* and *waaF6-R*. One of the PCR-positive colonies was selected and the constructed plasmid was named as pSW23T-*waaF6*. The plasmid was mobilized from the *E. coli* strain ω 7249/pSW23T-*waaF6* into *Y. pseudotuberculosis* strain No. 6 by conjugation. After 16 h mating on a LA plate supplemented with DAP the mating mix was collected into PBS, washed three times with PBS and aliquots plated on selective *Yersinia* agar plates supplemented with chloramphenicol. Chloramphenicol-resistant *Yersinia* transconjugants were recovered and checked for *waaF* complementation by DOC-PAGE.

SDS- or DOC-PAGE analysis and Western blotting

The bacteria were grown for 16–20 h at RT in 5 ml LB medium. The exact OD_{600} of the cultures was measured and 1 ml of the cultures was centrifuged. For DOC-PAGE, the pellets were resuspended in deoxycholate (DOC) lysis buffer [2% DOC, 4% 2-mercaptoethanol, 10% glycerol and 0.002% bromophenol blue in 1 M Tris-HCl buffer (pH 6.8)] in a volume adjusted according

to density of the culture (100 μ l/ OD_{600} = 1). For SDS-PAGE, the pellets treated as described previously.¹³ LPS phenotypes of proteinase K-treated whole-cell lysates were analyzed by silver-stained SDS or DOC-PAGE,^{13,32,33} and by Western blotting using rabbit anti-O:1b antiserum. The samples were transferred after DOC-PAGE from the gel onto a PVDF membrane by semidry blotter (Panther Semidry Electrobloetter; Owl Separation Systems, Thermo Scientific, Waltham, MA, USA) at 12 V, 22°C, for 2 h. After blocking 12–16 h at 4°C in 5% skimmed milk/1 \times Tris-buffered saline (TBS) Tween20 buffer (0.15 M NaCl, 10 mM Tris-HCl, 0.05% Tween20, pH 7.5), the membrane was incubated for 1 h at 22°C in a rolling tube with 1:1000–1:2000 diluted rabbit antisera in 5% skimmed milk/1 \times TBS Tween20 buffer. To detect the bound Abs, the membrane was incubated for 1 h at 22°C in a 1:2000-diluted HRP-conjugated secondary swine anti-rabbit Abs (DAKO, Glostrup, Denmark) in 5% skimmed milk/1 \times TBS Tween20 buffer. After washing, the secondary Abs were detected with the enhanced chemiluminescence solution (0.1 M Tris-HCl, 12.5 mM luminol, 2 mM coumaric acid, 0.03% H_2O_2) exposed to X-ray film (Kodak BioMax MR, Sigma-Aldrich, Helsinki, Finland).

Results and discussion

Purification and visualization of LPS from O:8 isolates

LPS was purified from *Y. pseudotuberculosis* O:8 isolates 151 and No. 6 using the hot phenol/water extraction procedure, and the sample was purified by enzymatic treatment, dialysis and ultracentrifugation, then lyophilized to remove contaminants (see 'Materials and methods').

Visualization of the LPS profiles revealed that the O:3 control has a single band of LPS (Figure 2). Consistent with our previous observation, the O:3 OPS chain could not be visualized as the periodate treatment in the staining process requires vicinal hydroxyl groups, which are rare in the O:3 structure.¹⁹ However, the O:3 band is as expected for lipid A with core oligosaccharide and one O unit. Both O:8 isolates produced bands with faster migration and presumably a lower molecular mass than the O:3 control. The LPS band of 151 runs faster than that of O:3, which is consistent with the previous serological classification that reported the isolate as rough.²⁰ However, the LPS band produced by No. 6 runs faster than that of 151 (Figure 2), indicating that the isolates are not the same, and the LPS is presumably significantly shorter.

Compositional analyses of LPS molecules from O:8 isolates

To determine the differences between the LPS of the two O:8 isolates, chemical analysis was performed on

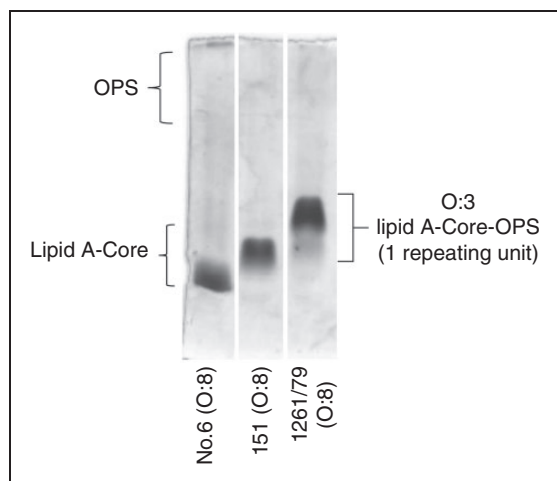


Figure 2. LPS profiles of *Y. pseudotuberculosis* serotype O:8 and O:3 isolates analyzed by DOC-PAGE.

purified LPS. The content of neutral sugars [Glc, Gal, L-glycero-D-manno-heptose (L,D-Hep) and D-glycero-D-manno-heptose (D,D-Hep)] was quantified according to the internal standard of Xyl and the values are given in nmol/mg LPS. Taken together, the compositional analyses of the LPS obtained from isolate No. 6 revealed the presence of phosphates (P), 3-deoxy-D-manno-oct-2-ulonic acid (Kdo), L,D-Hep (255 nmol/mg) and Glc (444 nmol/mg), which originated from a contamination as disclosed by NMR analysis of the O-deacylated LOS (*vide infra*). Isolate 151 was found to have additionally non-stoichiometric amounts of D,D-Hep (111 nmol/mg) and Gal (108 nmol/mg), a trace of glucosamine (GlcN), twice as much L,D-Hep (521 nmol/mg) as isolate No. 6 and high amounts of Glc (1164 nmol/mg), likely a contaminant as for strain No. 6., even though its presence on the core could not be excluded. Thus, strain 151 has some additional residues compared to No. 6 and this finding is consistent with the slower migration of its LPS, as shown in Figure 2.

Genetic analysis of the two strains provided insight into the mutations responsible for the phenotype observed.

Isolate 151 appears to have arisen from serotype O:4a

The OPS gene cluster of isolate 151 was sequenced (GenBank accession number KM454907) and found to have a gene cluster closely related to that of serotype O:4a, (GenBank accession number KJ504355).⁷ However, in comparison to O:4a, the remnant ISYps7 element in the 151 gene cluster is ~270 bp shorter at the end adjacent to *wzy* (Figure 3; Table S1), and the *ddhD* gene of strain 151 includes a frame-shift mutation 297 bp downstream of the start codon, which produces a premature stop codon 16 bp further downstream (Figure 3).

Serotype O:4a is known to produce smooth LPS that includes an O-unit main-chain structure containing D-GalpNAc and three D-Manp residues, with Tyvp attached to a D-Manp as a side-branch.³⁴ It is expected that the *ddhD* mutation in 151 would block synthesis of Tyvp, which would result in an O unit lacking the Tyvp side-branch. However, the SDS-PAGE analysis in Figure 2 is consistent with 151 being a rough strain with no O antigen at all. Additionally, no D-Manp residues were seen in the compositional analysis, further indicating absence of O antigen. This is not unexpected as O units lacking side-branch Tyv residues in *S. enterica* and *E. coli* are poorly translocated owing to Wzx specificity, and then are not available for ligation to lipid A core,^{35,36} and this may well apply to *Y. pseudotuberculosis*.

We used the O:4a *ddhD* gene to complement the mutation in 151, and observed that while production of long-chain O antigen was restored, the length was much less than that of O:4a LPS (Figure 4). Also, the lipid A core component of 151, with or without the cloned *ddhD* gene, ran faster than that of the O:4a wild type. The presence of sub-stoichiometric amounts of D,D-Hep and Gal in compositional analysis suggests that 151 might have also a mutation in *waaQ*, which would shorten the core and account for increased mobility. The O antigen is ligated to the Hep II (Figure 1), and the lower level of long-chain O antigen could be due to less efficient ligation to the modified core. Another possibility is that there is a polar effect of the *ddhD* mutation, as ribosomes would dissociate from the mRNA after the stop codon, 672 bp from the *ddhA* start codon, and translation of the next gene is assumed to be initiated by translational coupling.³⁷ We conclude that strain 151 has a mutation in the *ddhD* gene, and probably another in *waaQ*, resulting in the production of LPS with no O antigen and a truncated core. This accounts for the absence of epitope 9, which was not reported by Tsubokura and Aleksic.⁴ Epitope 20 is clearly not on the O antigen and is probably on part of the lipid A core exposed by the absence of O antigen. We have not sought to confirm the inferred core structure in strain 151, or suggested *waaQ* mutation, as the *ddhD* mutation is sufficient to account for the absence of O antigen which, as discussed below, appears to be all that is needed to form an O:8 strain.

Isolate No. 6 appears to have arisen from serotype O:1b

PCR genotyping, using the scheme described previously,²⁹ revealed that isolate No. 6 carried the O:1b gene cluster (data not shown). However, even though No. 6 still harbours the epitope 20, its LPS is deeply truncated and smaller than that observed for 151 (Figure 2), indicating the isolate probably has a

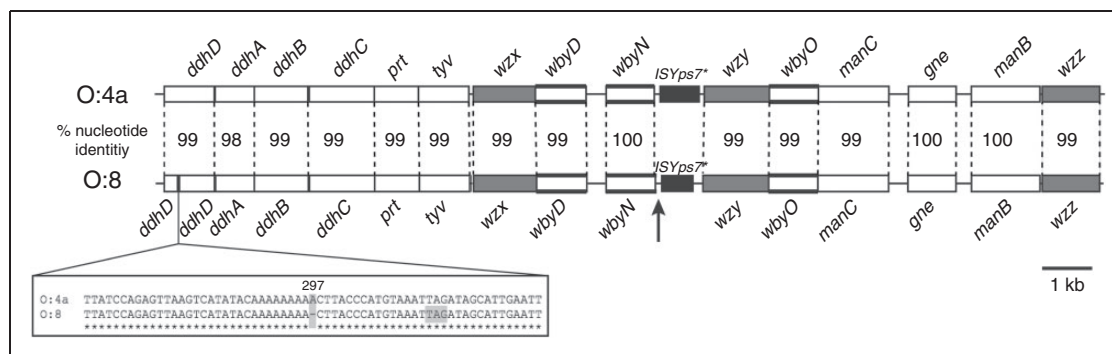


Figure 3. Comparison of the OPS gene clusters of O:8 and O:4a. All genes are oriented in the forward direction, and gene names are shown above or below. Genes that encode processing enzymes are gray, and bold horizontal lines indicate genes that encode glycosyltransferases. IS remnants are shown in black, and the vertical arrow indicates the position of a short repeat. Nucleotide sequence percentage identity levels are shown. The segment deleted in the O:8 *ddhD* gene is shown below. Figure is drawn to scale from GenBank accession numbers KJ504355 and KM454907.

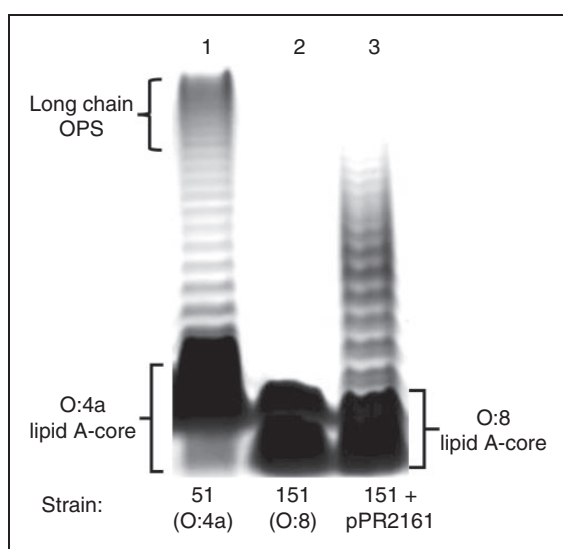


Figure 4. Complementations of *ddhD* in strain 151. Concentrated LPS was loaded into wells. Track 1 shows an SDS-PAGE gel of O:4a LPS, and tracks 2 and 3 LPS from O:8 strain 151 without and with complementation by a cloned *ddhD* gene.

mutation in the gene cluster responsible for core oligosaccharide synthesis.

Thus, structural analysis was performed on the LPS recovered from No. 6 because it contained already the structural elements of epitope 20, and to determine the extent of the LPS truncation to provide insights into the possible type of genetic mutation.

NMR spectroscopy of oligosaccharide phosphates isolated from No. 6

Mild hydrazinolysis of the LPS mixture from isolate No. 6 (57 mg) led to the *O*-deacylated products (42.2 mg; 76%) that were further subjected to strong alkaline

treatment in order to remove the amide-linked acyl residues. From this mixture (13.44 mg; 24% of the LPS), oligosaccharides **1**, **2** and **3** were isolated by HPAEC (2.4, 1.0 and 1.5 mg, 4.2, 1.75 and 2.7 % of the LPS, with retention time of 71.47, 79.76 and 85.00 min, respectively), representing the complete carbohydrate backbone of three different rough-type LPS molecules.

The complete assignment of ^1H and ^{13}C resonances of each oligosaccharide was achieved (Tables 2–4) by combining the information obtained from DQF-COSY, TOCSY, TROESY, HSQC, HMBC and HSQC-TOCSY NMR experiments, and started on oligosaccharide **3**, which is the least complex (Figure 5). This oligosaccharide presented two anomeric protons at 5.66 and 4.95 ppm, labelled **A** and **B**, and two couples of methylene protons at high field (2.13–1.76 ppm) related to the two Kdo units. Thus, **3** is a tetrasaccharide constituted by the two glucosamine units of the lipid A and two Kdo residues and its proton and carbon chemical shifts were similar to those of a similar oligosaccharide found in *E. coli* strain F515 and in *S. Minnesota* R595 (Table 4).³⁸ Combining the information of the 2D NMR experiments confirmed the structure reported from Zähringer et al.,³⁸ and structural assignment proceeded on the other oligosaccharides.

The ^1H -NMR spectrum of **1** (structure in Figure 6) presented one additional anomeric signal, **M**, at 5.35 ppm; for this residue the assignment of H-1 to H-4 proton and carbon chemical shifts was made by integrating information from COSY and TOCSY spectra. Analysis of the HMBC spectrum completed the assignment of this residue (Table 2): C-5 (74.1 ppm) was identified by virtue of its correlation with H-1 and H-3; in turn, H-5 showed a correlation, *inter alia*, with C-6 (70.4 ppm), while H-6 identified the C-7 of the residue (65.4 ppm). Indeed, **M** was the L,D-Hepp in agreement with chemical composition data; its

Table 2. 600-MHz ^1H and 150-MHz ^{13}C chemical shifts of **1** isolated by HPAEC chromatography, measured in $^2\text{H}_2\text{O}$ at 32°C with acetone as internal standard. HMBC spectrum detected further signals associated at Kdo and Kdo for which the anomeric carbons were found at 103.6 and 100.9 ppm, respectively. C-1 of Kdo was at 175.8 ppm, while that of Ko was not detected.

	1	2	3	4	5	6(a;b)	7(a;b)
6)- α -D-GlcpN-1P	5.67	3.42	3.92	3.58	4.16	4.29;3.77	—
A	92.1	55.7	70.8	70.9	73.8	70.7	—
6)- β -D-GlcpN-4P-(1 \rightarrow	4.90	3.10	3.88	3.81	3.74	3.71;3.47	—
B	100.7	56.8	73.2	75.4	75.4	63.6	—
α -L,D-Hepp	5.35	4.05	3.98	3.84	3.84	4.03	3.74 x2
M	102.3	71.5	71.2	67.5	74.1	70.4	65.3
	3(eq;ax)	4	5	6	7	8a;b	
α -Kdo-(2 \rightarrow	2.19;1.77	4.09	4.03	3.65	3.98	4.00;3.77	—
K_{ext}	35.8	67.4	67.6	73.9	71.8	64.6	—
4,5)- α -Kdo-(2 \rightarrow	2.05;1.98	4.21	4.27	3.72	3.83	3.88;3.66	—
K_{int}	35.6	70.8	74.3	73.2	70.7	64.9	—

Table 3. 600-MHz ^1H and 150-MHz ^{13}C chemical shifts of **2** isolated by HPAEC chromatography, measured in $^2\text{H}_2\text{O}$ at 32°C with acetone as internal standard. HMBC spectrum detected further signals associated at Ko and Kdo for which the anomeric carbons were found at 103.6 and 100.9 ppm, respectively. C-1 of Kdo was at 175.8 ppm, while that of Ko was not detected.

	1	2	3	4	5	6(a;b)	7(a;b)
6)- α -D-GlcpN-1P	5.65	3.40	3.91	3.63	4.17	4.32;3.78	—
A	91.9	55.9	71.0	70.9	73.6	71.0	—
6)- β -D-GlcpN-4P-(1 \rightarrow	4.88	3.06	3.85	3.75	Ca. 4.00	3.72;3.59	—
B	100.9	56.9	73.8	74.6	75.6	63.7	—
α -L,D-Hepp	5.36	4.07	3.98	3.84	3.80	4.024	3.75;3.69
M	102.2	71.4	71.6	67.5	74.0	70.4	65.4
	3(eq;ax)	4	5	6	7	8a;b	
α -Ko-(2 \rightarrow	4.08	3.99	4.11	3.68	4.09	4.04;3.80	—
Ko	73.2	67.5	69.7	73.8	71.3	64.5	—
4,5)- α -Kdo-(2 \rightarrow	2.09;1.99	4.20	4.24	3.75	3.83	3.89;3.69	—
K	35.6	71.7	73.8	73.1	70.6	64.7	—

Table 4. 600-MHz ^1H and 150-MHz ^{13}C chemical shifts of **3** isolated by HPAEC chromatography, measured in $^2\text{H}_2\text{O}$ at 25°C with acetone as internal standard. HMBC spectrum detected further signals associated at Kdo_{int} and Kdo_{ext} for which the anomeric carbons were found at 101.0 and 100.8 ppm, while C-1 were at 176.2 and 177.0, respectively.

	1	2	3	4	5	6a;b
6)- α -D-GlcpN-1P	5.66	3.40	3.90	3.53	4.16	4.27;3.73
A	91.9	55.7	70.9	71.1	73.9	70.7
6)- β -D-GlcpN-4P-(1 \rightarrow	4.95	3.07	3.87	3.80	3.73	3.48;3.75
B	100.7	56.8	73.3	75.1	75.4	63.5
	3(eq;ax)	4	5	6	7	8a;b
α -Kdo-(2 \rightarrow	2.13;1.76	4.07	4.04	3.59	3.98	4.01;3.74
K_{ext}	35.7	67.2	67.4	74.0	71.0	64.6
4)- α -Kdo-(2 \rightarrow	1.99;1.93	4.13	4.13	3.76	3.91	3.91;3.65
K_{int}	34.7	69.8	65.7	72.6	70.9	64.6

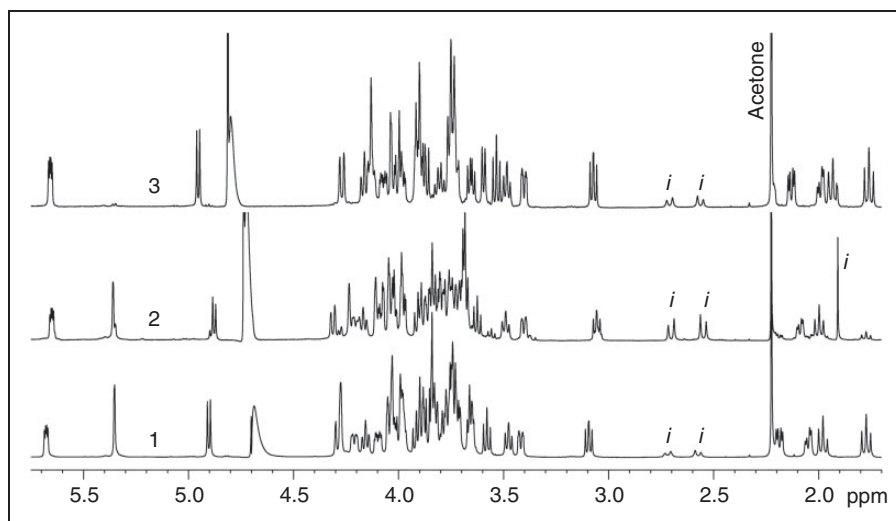


Figure 5. ^1H NMR spectra of **1**, **2** and **3** purified via HPAEC. Spectra are calibrated with respect to internal acetone and measured at 32°C (**1** and **2**) or at 25°C, as for **3**. Impurities are marked with “i”.

anomeric configuration was α , as evaluated by the anomeric $^1J_{\text{C,H}}$ value (170.8 Hz) as observed for the anomeric signal in the HMBC spectrum.

As for **2**, its anomeric region was similar to that of **1**, but the high-field region presented only one couple of methylene protons, suggesting the occurrence of only one Kdo residue. Attribution of all proton and carbon chemical shifts was performed as illustrated for **1** and **3** (Table 3), and the Kdo residue (**K**) was identified as an internal unit substituted at both O-4 and O-5. Importantly, the modest glycosylation shift observed for C-4 suggested the occurrence of a ketose other than Kdo at this position.

Consistent with this, H-3_{eq} of **K** (2.09 ppm) gave a medium nuclear overhauser effect (NOE) with a proton at 3.68 ppm, which, in turn, correlated with a proton at 4.09 ppm in the COSY spectrum. This last proton displayed one additional cross peak in the HSQC-TOCSY spectrum with a hydromethyl group at 64.5 ppm (Figure 7), along with its direct carbon correlation and with the carbon associated to the proton found previously at 3.68 ppm. Other information derived from TROESY spectrum analysis revealed that the proton at 3.68 displayed one strong and one medium NOE with the protons at 4.11 and 3.99 ppm, respectively, as displayed for Kdo residue. Last, the HSQC-TOCSY spectrum proved that these two protons correlated with an additional proton/carbon signal at 4.08/73.2 ppm (Figure 7), which, in turn, correlated with a carbon at 103.6 ppm, as shown in the HMBC spectrum. Taking all this information together, occurrence of an octulosonic acid was proposed and confirmed by comparison of the chemical shifts of this residue with those of Ko.³⁹ Hence, the complete structure of **2** was also defined (Figure 6). The structure is the same as reported for the inner core of *Y. pestis*, in effect a clone of *Y. pseudotuberculosis*.¹⁶

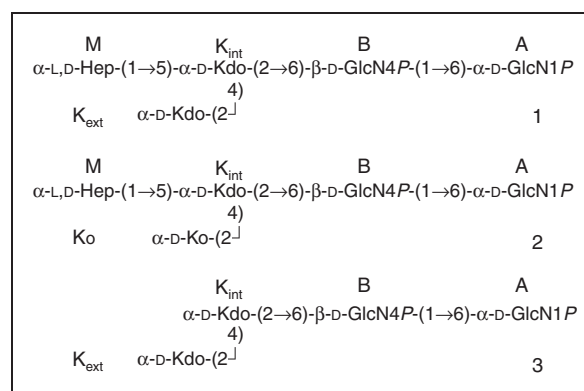


Figure 6. Structures of **1**, **2** and **3** isolated from *Y. pseudotuberculosis* O:8 after full de-lipidation and HPAEC. Letters reflect those used in NMR assignment.

ESI-MS/IT-TOF analysis

ESI-MS spectra of **1**, **2** and **3** were acquired and spectra in negative mode were more informative than those in positive mode (Figure 8). The charge-deconvoluted ESI-MS spectra (not shown) gave the molecular ions of **1** and **2** at m/z 1132.26 and 1148.25, respectively, which were consistent with the composition $\text{GlcN}_2\text{P}_2\text{Kdo}_2\text{Hep}$ and $\text{GlcN}_2\text{P}_2\text{KdoKoHep}$, in agreement with the NMR data. As for **3**, the ESI-MS spectrum yielded one small signal at m/z 939.19 attributed to $[\text{M-H}]^-$ of $(\text{GlcN})_2\text{P}_2\text{Kdo}_2$ (Figure 8). As this spectrum did not contain the double-charged species, deconvolution was not applied. To confirm the compositional details, the ESI-IT-TOF MS/MS spectra were acquired for **1** and **2** selecting for each oligosaccharide the double-negatively charged signal as parent ion (Figure 9).

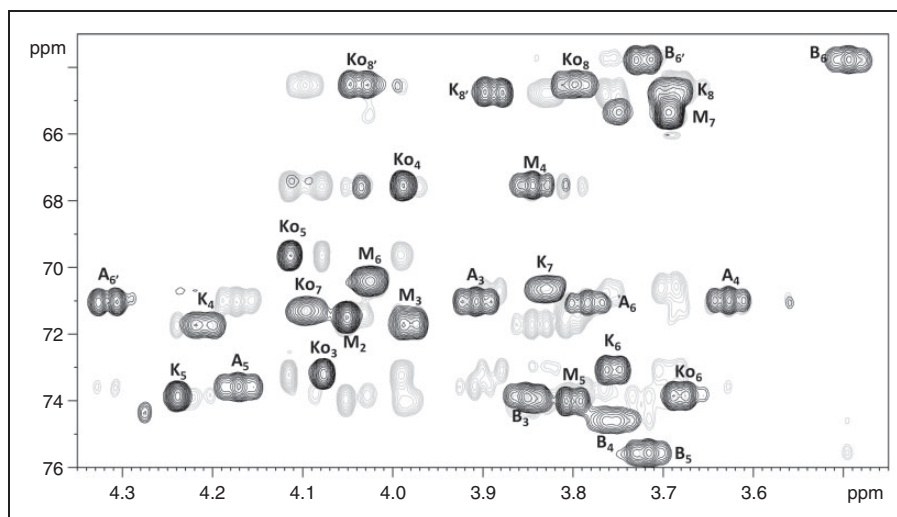


Figure 7. Expansion of HSQC (black) and HSQC-TOCSY (grey) spectrum of **2** from *Y. pseudotuberculosis* O:8 (600 MHz, 32°C, $^2\text{H}_2\text{O}$). Labels refer to the HSQC spectrum densities and are those used in Table 3.

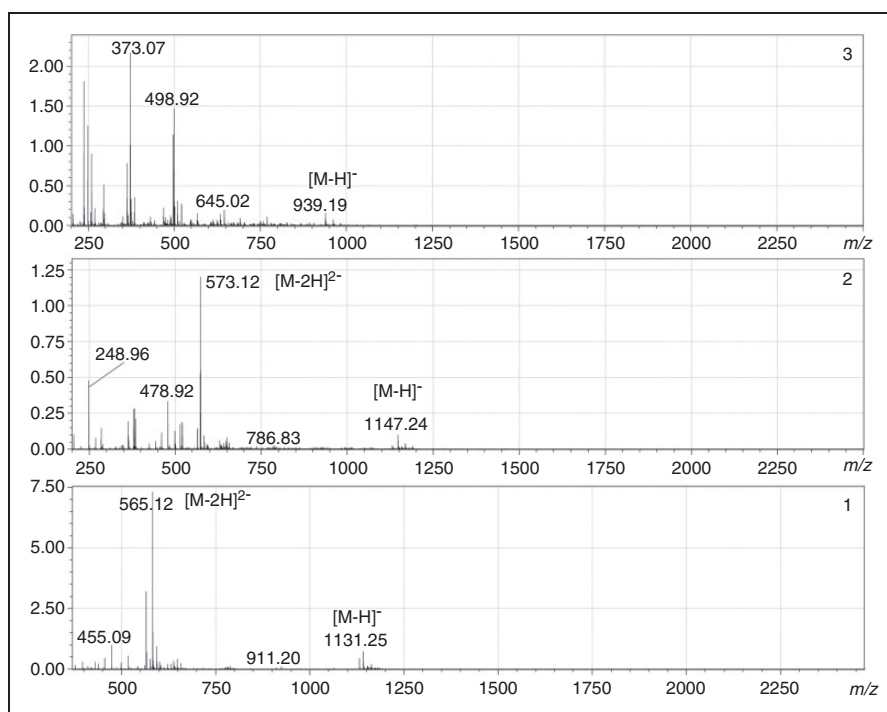


Figure 8. ESI-MS spectra in negative mode of **1**, **2** and **3** obtained after HPAEC purification. Ordinate axis reports the ion abundance scaled at 10^6 .

The MS/MS spectrum (negative ion mode) of **1** showed intense fragments at m/z 911.19, 499.07 and 631.07 (Figure 9, bottom). The first signal was attributed to the complete oligosaccharide oxonium ion devoid of the terminal Kdo, that is, a Y ion, according to the fragmentation rules.⁴⁰ Likewise, m/z 499.07 was a Y fragment containing the two phosphorylated GlcN, while m/z 631.17 was the complimentary B ion. The ion at m/z 401.11 originated from that at m/z 499.07 by loss of a phosphate ion. The MS/MS spectrum of **2** displayed the

same fragmentation pattern described for **1** (Figure 9), with the difference that no loss of the Ko residue occurred, probably owing to the higher stability of its glycosidic linkage compared with that of Kdo.

LPS truncation in No. 6 is the result of a mutation in waaF

The core oligosaccharides of *Enterobacteriaceae* species usually include three Hep residues (Hep I, Hep II and

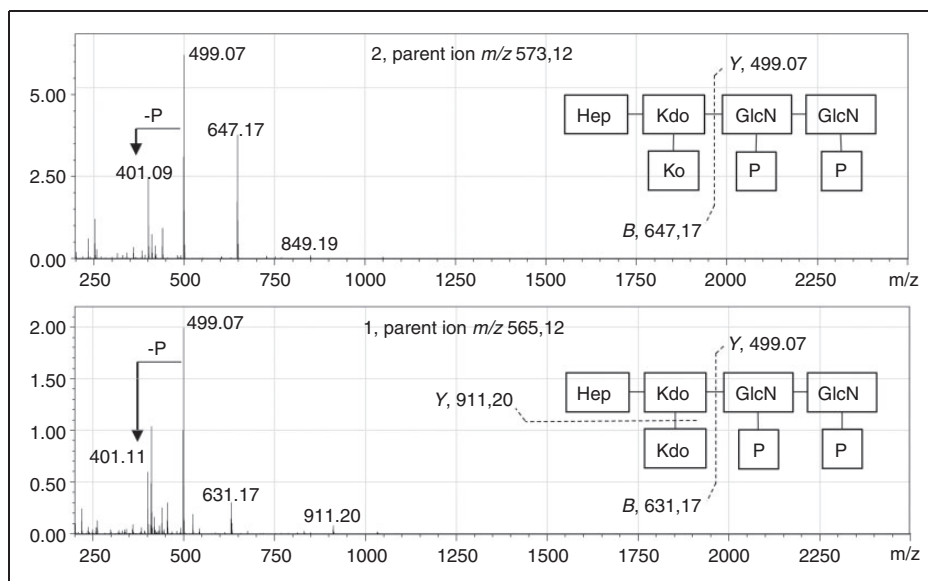


Figure 9. ESI-MS MS/MS spectra of the fully de-lipidated oligosaccharides **1** (bottom) and **2** (top). For each oligosaccharide, the double-charged ion was selected as parent ion; main fragments are indicated in the structure of the inset: italic letters refer to the fragmentation pathway of the oligosaccharide as described.⁴⁰ Ordinate axis reports the ion abundance scaled at 10^6 .

Hep III) and three Hexp residues (Hex I, Hex II and Hex III).⁴¹ However, while the three truncated LPS forms obtained from isolate No. 6 contained a normal lipid A component substituted with Kdo-Ko moieties, two of the forms had only a single L,D-Hexp residue (Hep I) mounted to Kdo (Figure 6). As Hep I is present in two of the structures, the rough nature of the LPS cannot be attributed to a defect in the ADP-Hep biosynthesis pathway. However, the inability to add Hep II to Hep I indicates a defect in the activity of the WaaF heptosyltransferase II, which would prevent further additions to the core oligosaccharide, including glucose at Hep I,⁴² presumably because the Glc transferase requires Hep II residue in the acceptor. The structure is the same as that reported for a *waaF* mutation in *Y. pestis*,⁴³ and has a similar LPS profile to *Y. enterocolitica* O:3 *waaF* mutant, M164 (*waaF::CatMu*), when visualized by silver staining (Figure 10A).

Sequencing of the *waaF* gene in No. 6 revealed a 53-bp deletion in the middle of the gene causing a frame shift and truncation of the gene product by about 160 C-terminal amino acids. As the *waaF* gene is a middle gene in a three-gene *waa* operon, we cloned the entire operon from serotype O:1b (isolate IP32953) to create plasmid pSW23T-*waaF*6, and used it to complement isolate No. 6. Complementation resulted in the restoration of the LPS core band to a size equivalent to that of serotype O:1b (Figure 10A). However, the complemented strain failed to show the O:1b-specific O antigen in Western blotting, indicating that strain No. 6 may additionally carry a second mutation in the O antigen gene cluster (Figure 10B). The nature of the second mutation was not addressed, as the deletion in *waaF*

was sufficient to cause the truncation of LPS, and explained the origin of this O:8 strain.

Final comments

The two O:8 strains studied have different origins as shown by the O-antigen genes present, and we propose that epitope 20 is on a structure that is masked by O antigen, as both strains are rough mutants.

The two O:8 strains studied both have rough LPS, as reported previously for type strain 151. It is well established that under normal laboratory conditions many bacteria, including *Y. pseudotuberculosis*, accumulate point mutations in the OPS gene cluster that change the colony morphology from smooth to rough. In a wild type bacterium, the cell surface includes a heterogeneous population of LPS molecules with some containing lipid A and core oligosaccharide only, while others include either OPS or a single O unit. Thus, when the serotyping scheme for *Y. pseudotuberculosis* was developed, the antisera typically contained anti-core Abs that were removed when the antisera were cross-absorbed with bacteria of other serotypes.

In the last update to the scheme, the anti-O:8 antiserum was reported to also react with O:2c and O:4a bacteria,⁴ and our analysis of the 151 strain that was used for this showed that it had an O:4a gene cluster and that a mutation in the *ddhD* gene of that gene cluster conferred the rough phenotype. The No. 6 strain is a more typical rough strain with a mutation in *waaF* that blocks completion of the inner core.

Here we have provided evidence that the two *Y. pseudotuberculosis* serotype O:8 isolates assessed in this study, are spontaneous mutants of other validated

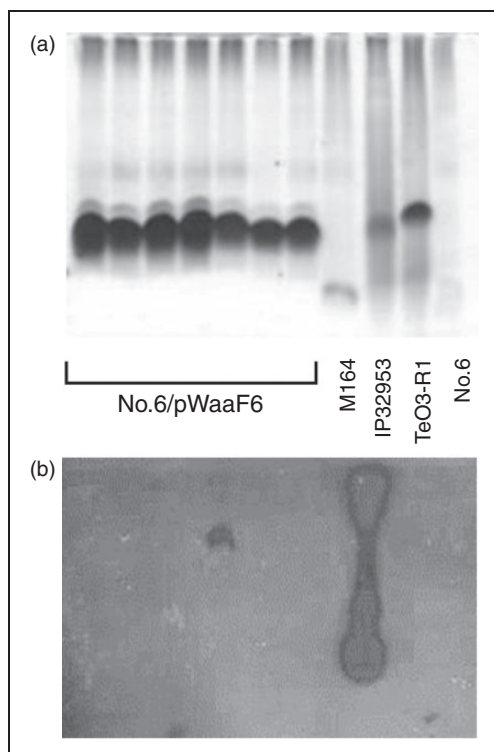


Figure 10. Complementation of loss of WaaF function in strain No. 6 by the *waaDFC* operon. (A) Silver staining of LPS samples separated in DOC-PAGE. (B) Western blotting of the same samples using rabbit antiserum specific for *Y. pseudotuberculosis* serotype O:1b. The LPS samples loaded to the lanes are identified between the panels: No. 6/pWaaF6 = seven independent clones of the No. 6 strain complemented with *waaDFC* operon using plasmid pSW23T-waaF6; M164 = *Y. enterocolitica* strain YeO3-R1-M164, a *waaF::CatMu* mutant;⁴² IP32953 = *Y. pseudotuberculosis* O:1b strain IP32953;⁴⁵ YeO3-R1 = *Y. enterocolitica* O:3 spontaneous rough mutant;⁴⁷ No. 6 = *Y. pseudotuberculosis* strain No. 6.

serotypes. It is interesting that both appear to have separate mutations affecting the O antigen and the LPS core. For 151 the mutation in *ddhD* would make the strain rough but did not explain the data obtained later on the core composition, which must be due to a separate mutation, probably in *waaQ*. For No. 6, the LPS composition data showed that the core was defective and so the O-antigen gene cluster was not sequenced. But later data showed that restoration of the core structure did not rescue O-antigen expression, probably because there is a mutation in the O-antigen gene cluster. The presence of two mutations in both strains is unlikely to be a coincidence. However, it is not surprising as mutants making incomplete O antigen are often deleterious and leads to further mutations. This phenomenon is not well understood, and falls outside of the scope of this study. However, these findings do show that serotype O:8 is not due to presence of a specific form of O antigen, and epitope 20 should be removed from the serotyping scheme, bringing the total

number to 20 serotypes for the *Y. pseudotuberculosis* complex. The fact that the ancestral strains were of different serotypes indicates that it is being rough that exposes epitope 20, which is present but not exposed in the ancestral strains. In these circumstances there is no reason to further explore the nature of the mutations in the 151 core or the No 6 O-antigen gene cluster, but the nature of epitope 20 is a topic for future research.

Acknowledgements

The authors thank Sylvia Düpow (RCB) for technical assistance. JK was supported by an Australian Postgraduate Award (APA).

Declaration of Conflicting Interests

The author(s) declared no potential conflicts of interest with respect to the research, authorship, and/or publication of this article.

Funding

The author(s) received no financial support for the research, authorship, and/or publication of this article.

References

1. Ho N, Kondakova AN, Knirel YA, et al. The biosynthesis and biological role of 6-deoxyheptose in the lipopolysaccharide O-antigen of *Yersinia pseudotuberculosis*. *Mol Microbiol* 2008; 68: 424–447.
2. Mecsas J, Bilis I and Falkow S. Identification of attenuated *Yersinia pseudotuberculosis* strains and characterization of an orogastric infection in BALB/c mice on day 5 postinfection by signature-tagged mutagenesis. *Infect Immun* 2001; 69: 2779–2787.
3. Porat R, McCabe WR and Brubaker RR. Lipopolysaccharide-associated resistance to killing of yersiniae by complement. *J Endotox Res* 1995; 2: 91–97.
4. Tsubokura M and Aleksic S. A simplified antigenic scheme for serotyping of *Yersinia pseudotuberculosis*: phenotypic characterization of reference strains and preparation of O and H factor sera. *Contrib Microbiol Immunol* 1995; 13: 99–105.
5. Laukkanen-Ninios R, Didelot X, Jolley KA, et al. Population structure of the *Yersinia pseudotuberculosis* complex according to multilocus sequence typing. *Environmental Microbiol* 2011; 13: 3114–3127.
6. Savin C, Martin L, Bouchier C, et al. The *Yersinia pseudotuberculosis* complex: characterization and delineation of a new species, *Yersinia wautersii*. *Int J Med Microbiol* 2014; 304: 452–463.
7. Reeves PR, Pacinelli E and Wang L. O antigen gene clusters of *Yersinia pseudotuberculosis*. *Adv Exp Med Biol* 2003; 529: 199–206.
8. Bacterial Carbohydrate Structure Database. Available at: <http://csdb.glycoscience.ru/bacterial/> (accessed 27 January 2006).
9. Knirel YA. Structure of O-antigens. In: Valvano MA and Knirel YA (eds) *Bacterial lipopolysaccharide*. Vienna: Springer Verlag, 2011, pp.41–115.
10. Reeves PR, Cunneen MM, Liu B, et al. Genetics and evolution of the *Salmonella* galactose-initiated set of O antigens. *PLoS One* 2013; 8: e69306.
11. Cunneen MM, Liu B, Wang L, et al. Biosynthesis of UDP-GlcNAc, UndPP-GlcNAc and UDP-GlcNAcA involves three easily distinguished 4-epimerase enzymes, Gne, Gnu and GnaB. *PLoS One* 2013; 8: e67646.

12. Rush JS, Alaimo C, Robbiani R, et al. A novel epimerase that converts GlcNAc-P-P-undecaprenol to GalNAc-P-P-undecaprenol in *Escherichia coli* O157. *J Biol Chem* 2010; 285: 1671–1680.
13. Kenyon JJ and Reeves PR. The Wzy O-antigen polymerase of *Yersinia pseudotuberculosis* O:2a has a dependence on the Wzz chain-length determinant for efficient polymerization. *FEMS Microbiol Lett* 2013; 349: 163–170.
14. Achtman M, Zurth K, Morelli G, et al. *Yersinia pestis*, the cause of plague, is a recently emerged clone of *Yersinia pseudotuberculosis*. *Proc Natl Acad Sci U S A* 1999; 96: 14043–14048.
15. Miller SI, Ernst RK and Bader MW. LPS, TLR4 and infectious disease diversity. *Nat Rev Microbiol* 2005; 3: 36–46.
16. Knirel YA and Anisimov AP. Lipopolysaccharide of *Yersinia pestis*, the cause of plague: structure, genetics, biological properties. *Acta Naturae* 2012; 4: 46–58.
17. Knirel YA, Kondakova AN, Bystrova OV, et al. New features of *Yersinia* lipopolysaccharide structure as revealed by high-resolution electrospray ionization mass spectrometry. *Adv Sci Lett* 2008; 1: 192–198.
18. Tsubokura M, Otsuki K, Kawaoka Y, et al. Addition of new serogroups and improvement of the antigenic designs of *Yersinia pseudotuberculosis*. *Curr Microbiol* 1984; 11: 89–92.
19. Aleksic S, Suchan G, Bockemühl J, et al. An extended antigenic scheme for *Yersinia pseudotuberculosis*. In: Une T, Maruyama T and Tsubokura M (eds) *Current investigations of the microbiology of Yersiniae. Contributions to microbiology and immunology*. Vol 12, Basel: Karger, 1991, pp.235–238.
20. Tsubokura M, Aleksic S, Fukushima H, et al. Characterization of *Yersinia pseudotuberculosis* Serogroups O9, O10 and O11; Subdivision of O1 Serogroup into O1a, O1b, and O1c Subgroups. *Zentralbl Bakteriell* 1993; 278: 500–509.
21. De Castro C, Skurnik M, Molinaro A, et al. Characterization of the O-polysaccharide structure and biosynthetic gene cluster of *Yersinia pseudotuberculosis* serotype O:15. *Innate Immun* 2009; 15: 351–359.
22. Westphal O and Jann K. Bacterial lipopolysaccharides extraction with phenolwater and further applications of the procedure. *Methods Carbohydr Chem* 1965; 5: 83–91.
23. De Castro C, Parrilli M, Holst O, et al. Microbe-associated molecular patterns in innate immunity: extraction and chemical analysis of Gram-negative bacterial lipopolysaccharides. *Methods Enzymol* 2010; 480: 89–115.
24. Brade H, Galanos C and Lüderitz O. Differential determination of the 3-deoxy-D-mannooctulosonic acid residues in lipopolysaccharides of *Salmonella minnesota* rough mutants. *Eur J Biochem* 1983; 131: 195–200.
25. Kaca W, de Jongh-Leuvenink J, Zähringer U, et al. Isolation and chemical analysis of 7-O-(2-amino-2-deoxy- α -D-glucopyranosyl)-L-glycero-D-manno-heptose as a constituent of the lipopolysaccharides of the UDP-galactose epimerase-less mutant J-5 of *Escherichia coli* and *Vibrio cholerae*. *Carbohydr Res* 1988; 179: 289–299.
26. Duda KA, Lindner B, Brade H, et al. The lipopolysaccharide of the mastitis isolate *Escherichia coli* strain 1303 comprises a novel O-antigen and the rare K-12 core type. *Microbiology* 2011; 157: 1750–1760.
27. Holst O. Deacylation of lipopolysaccharides and isolation of oligosaccharide phosphates. In: Holst O (ed.) *Methods in molecular biology, bacterial toxins: methods and protocols*. Totowa, NJ: Humana Press, 2000, pp.345–353.
28. De Castro C, Kenyon JJ, Cunneen MM, et al. The O-specific polysaccharide structure and gene cluster of serotype O:12 of the *Yersinia pseudotuberculosis* complex, and the identification of a novel L-quinovose biosynthesis gene. *Glycobiol* 2013; 23: 346–353.
29. Bogdanovich T, Carniel E, Fukushima H, et al. Use of O-antigen gene cluster-specific PCRs for the identification and O-genotyping of *Yersinia pseudotuberculosis* and *Yersinia pestis*. *J Clin Microbiol* 2003; 41: 5103–5112.
30. Amann E, Ochs B and Abel KJ. Tightly regulated *tac* promoter vectors useful for the expression of unfused and fused proteins in *Escherichia coli*. *Gene* 1988; 69: 301–315.
31. Demarre G, Guerout AM, Matsumoto-Mashimo C, et al. A new family of mobilizable suicide plasmids based on broad host range R388 plasmid (IncW) and RP4 plasmid (IncPalpha) conjugative machineries and their cognate *Escherichia coli* host strains. *Res Microbiol* 2005; 156: 245–255.
32. Skurnik M, Venho R, Toivanen P, et al. A novel locus of *Yersinia enterocolitica* serotype O-3 involved in lipopolysaccharide outer core biosynthesis. *Mol Microbiol* 1995; 17: 575–594.
33. Zhang L, Al-Hendy A, Toivanen P, et al. Genetic organization and sequence of the *rfb* gene cluster of *Yersinia enterocolitica* serotype O:3: similarities to the dTDP-L-rhamnose biosynthesis pathway of *Salmonella* and to the bacterial polysaccharide transport systems. *Mol Microbiol* 1993; 9: 309–321.
34. Kondakova AN, Bystrova OV, Shaikhutdinova RZ, et al. Structure of the O-antigen of *Yersinia pseudotuberculosis* O:4a revised. *Carbohydr Res* 2009; 344: 531–534.
35. Hong Y, Cunneen MM and Reeves P. The Wzx translocases for *Salmonella enterica* O-antigen processing have unexpected serotype specificity. *Mol Microbiol* 2012; 84: 620–623.
36. Hong Y and Reeves PR. Diversity of O-antigen repeat unit structures can account for the substantial sequence variation of Wzx translocases. *J Bacteriol* 2014; 196: 1713–1722.
37. Levin-Karp A, Barenholz U, Bareia T, et al. Quantifying translational coupling in *E. coli* synthetic operons using RBS modulation and fluorescent reporters. *ACS Synth Biol* 2013; 2: 327–336.
38. Zähringer U, Sinnwell V, Peter-Katalinic J, et al. Isolation and characterization of the tetrasaccharide (bis)phosphate from the glycosyl backbone of *Salmonella minnesota* and *Escherichia coli* re-mutant lipopolysaccharides. *Tetrahedron* 1993; 49: 4193–4200.
39. Isshiki Y, Kawahara K and Zähringer U. Isolation and characterisation of disodium (4-amino-4-deoxy- β -L-arabinopyranosyl)-(1 \rightarrow 8)-(D-glycero- α -D-talo-oct-2-ulopyranosyl)- (2 \rightarrow 4)-(methyl-3-deoxy-D-manno-oct-2-ulopyranosidionate) from the lipopolysaccharide of *Burkholderia cepacia*. *Carbohydr Res* 1998; 313: 21–27.
40. Domon B and Costello CE. A systematic nomenclature for carbohydrate fragmentations in FAB-MS/MS spectra of glycoconjugates. *Glycoconjugate J* 1988; 5: 397–409.
41. Heinrichs DE, Yethon JA and Whitfield C. Molecular basis for structural diversity in the core regions of the lipopolysaccharides of *Escherichia coli* and *Salmonella enterica*. *Mol Microbiol* 2002; 30: 221–232.
42. Noszczyńska M, Kasperkiewicz K, Duda KA, et al. Serological characterization of the enterobacterial common antigen substitution of the lipopolysaccharide of *Yersinia enterocolitica* O:3. *Microbiol* 2015; 161: 219–227.
43. Anisimov AP, Dentovskaya SV, Kondakova AN, et al. *Yersinia pestis* lipopolysaccharide in host-pathogen interactions. In: Shafferman A, Ordentlich A and Velan B (eds) *The Challenge of highly pathogenic microorganism*. Dordrecht: Springer Netherlands, 2010, pp.77–87.
44. Skurnik M. Lack of correlation between the presence of plasmids and fimbriae in *Yersinia enterocolitica* and *Yersinia pseudotuberculosis*. *J Appl Bact* 1984; 56: 355–363.
45. Chain PS, Carniel E, Larimer FW, et al. Insights into the evolution of *Yersinia pestis* through whole-genome comparison with *Yersinia pseudotuberculosis*. *Proc Natl Acad Sci U S A* 2004; 101: 13826–13831.
46. Babic A, Guerout AM and Mazel D. Construction of an improved RP4 (RK2)-based conjugative system. *Res Microbiol* 2008; 159: 545–549.
47. Al-Hendy A, Toivanen P and Skurnik M. Lipopolysaccharide O side chain of *Yersinia enterocolitica* O:3 is an essential virulence factor in an orally infected murine model. *Infect Immun* 1992; 60: 870–875.